



An in vivo RNAi screen uncovers the role of AdoR signaling and adenosine deaminase in controlling intestinal stem cell activity

Chiwei Xu^a, Brian Franklin^a, Hong-Wen Tang^a, Yannik Regimbald-Dumas^b, Yanhui Hu^a, Justine Ramos^a, Justin A. Bosch^a, Christians Villalta^a, Xi He^b, and Norbert Perrimon^{a,c,1}

^aDepartment of Genetics, Blavatnik Institute, Harvard Medical School, Boston, MA 02115; ^bF. M. Kirby Neurobiology Center, Boston Children's Hospital, Harvard Medical School, Boston, MA 02115; and ^cHoward Hughes Medical Institute, Harvard Medical School, Boston, MA 02115

Contributed by Norbert Perrimon, November 15, 2019 (sent for review January 9, 2019; reviewed by Utpal Bannerjee and Heinrich Jasper)

Metabolites are increasingly appreciated for their roles as signaling molecules. To dissect the roles of metabolites, it is essential to understand their signaling pathways and their enzymatic regulations. From an RNA interference (RNAi) screen for regulators of intestinal stem cell (ISC) activity in the *Drosophila* midgut, we identified adenosine receptor (*AdoR*) as a top candidate gene required for ISC proliferation. We demonstrate that Ras/MAPK and Protein Kinase A (PKA) signaling act downstream of *AdoR* and that Ras/MAPK mediates the major effect of *AdoR* on ISC proliferation. Extracellular adenosine, the ligand for *AdoR*, is a small metabolite that can be released by various cell types and degraded in the extracellular space by secreted adenosine deaminase. Interestingly, down-regulation of adenosine deaminase-related growth factor A (*Adgf-A*) from enterocytes is necessary for extracellular adenosine to activate *AdoR* and induce ISC overproliferation. As *Adgf-A* expression and its enzymatic activity decrease following tissue damage, our study provides important insights into how the enzymatic regulation of extracellular adenosine levels under tissue-damage conditions facilitates ISC proliferation.

adenosine receptor | adenosine deaminase | intestinal stem cell | RNAi screen

The *Drosophila* midgut epithelium consists of multipotent intestinal stem cell (ISCs), their immediate progenies known as enteroblasts (EBs, which are progenitor cells primed for differentiation), and differentiated cells including enterocytes (ECs, which is the major cell type in number), and enteroendocrine cells (EEs) (1, 2). ISCs/EBs can adjust their proliferation and differentiation activities by deploying conserved core pathways such as JAK/Stat, Notch, Ras/MAPK, JNK, and Hippo (3). The dynamic responses of adult ISCs/EBs to different regenerative demands under physiological or pathological conditions (4) depend on the machineries to detect microenvironment cues and modulate the activity of aforementioned core pathways, which have not been investigated in vivo systematically.

To understand how ISCs/EBs sense their microenvironment, we performed an RNAi screen to identify receptor-coding genes that regulate ISC activity, among which *Adenosine Receptor* (*AdoR*) emerged as a top candidate required for ISC self-renewal and proliferation. Characterization of the *AdoR*-signaling pathway revealed the role of *AdoR* downstream pathways in regulating different aspects of ISC activity. Importantly, we demonstrate that the mitogenic activity of the *AdoR* ligand, adenosine, is inhibited by *adenosine deaminase-related growth factor A* (*Adgf-A*) from ECs and that *Adgf-A* activity decreases following tissue damage. Altogether, our study demonstrates how an EC-derived metabolic enzyme modulates ISC activity by restricting extracellular adenosine.

Results

A Receptome-Wide RNA Interference Screen Identifies Regulators of ISC Activity. Precise control of stem cell activity is important for tissue homeostasis and tumor prevention. To systematically analyze how ISCs respond to and process signals from the

microenvironment, we performed an RNA interference (RNAi) screen to identify transmembrane and nuclear receptors implicated in ISC/EB regulation. RNAi lines were crossed to the *EGT* driver, whereby the endogenous enhancer of *escargot* (*esg*) drives expression in ISCs/EBs and *tubGal80^{ts}* allows temporal control of Gal4 activity (2). As the screen readout, we developed a quantitative assay measuring *EGT*-driven luciferase (Luc) activity as a proxy for ISC/EB abundance (Fig. 1A and Dataset S1 A–E). We identified 350 *Drosophila* genes which are orthologous to human genes and encode known or putative receptors as our candidates (Dataset S1F). We used 525 UAS-RNAi fly stocks to knock down each gene in adult ISCs/EBs (Dataset S1F). In addition to measuring normally fed flies, we also performed the screen when flies were fed with bleomycin to stimulate ISC proliferation (4). The top hits were validated by additional reagents [RNAi, short guide RNA (sgRNA), mutant, etc.] and further characterized by immunostainings for the ISC marker D-lacZ and the mitosis marker phosphohistone H3 (pH3) (SI Appendix, Fig. S1 A–X and Dataset S1G).

Results from the screen confirmed the known effects of core signaling pathway receptors. For example, knockdowns of *EGFR* and *InR*, which encode receptors required for ISC proliferation (5, 6), cause a decrease in ISC/EB number (Fig. 1B). In contrast, knockdown of *dome* or *N*, which encodes the JAK/Stat or Notch pathway receptor required for ISC differentiation (1, 2, 7), increases ISC/EB number (Fig. 1B). Although the lists of ISC regulators under normal feeding and tissue-damage conditions largely overlap, we also identified regulators that preferentially

Significance

Regulation of stem cells by microenvironment signals is important to maintain epithelial homeostasis. Using a quantitative readout, we screened for receptor genes that affect the intestinal stem cell pool size in the adult *Drosophila* midgut. The top candidate of our screen, *AdoR*, underscores the importance of purinergic signaling in controlling ISC activity. Furthermore, we identified a pivotal role of an enterocyte-derived metabolic enzyme, *Adgf-A*, in limiting the activity of extracellular adenosine and shaping the ISC microenvironment.

Author contributions: C.X. and N.P. designed research; C.X., B.F., H.-W.T., Y.R.-D., and J.R. performed research; J.A.B. and C.V. contributed new reagents/analytic tools; C.X., Y.R.-D., Y.H., X.H., and N.P. analyzed data; and C.X. and N.P. wrote the paper.

Reviewers: U.B., University of California, Los Angeles; and H.J., Buck Institute for Research on Aging.

The authors declare no competing interest.

Published under the PNAS license.

¹To whom correspondence may be addressed. Email: perrimon@genetics.med.harvard.edu.

This article contains supporting information online at <https://www.pnas.org/lookup/suppl/doi:10.1073/pnas.1900103117/-DCSupplemental>.

First published December 18, 2019.

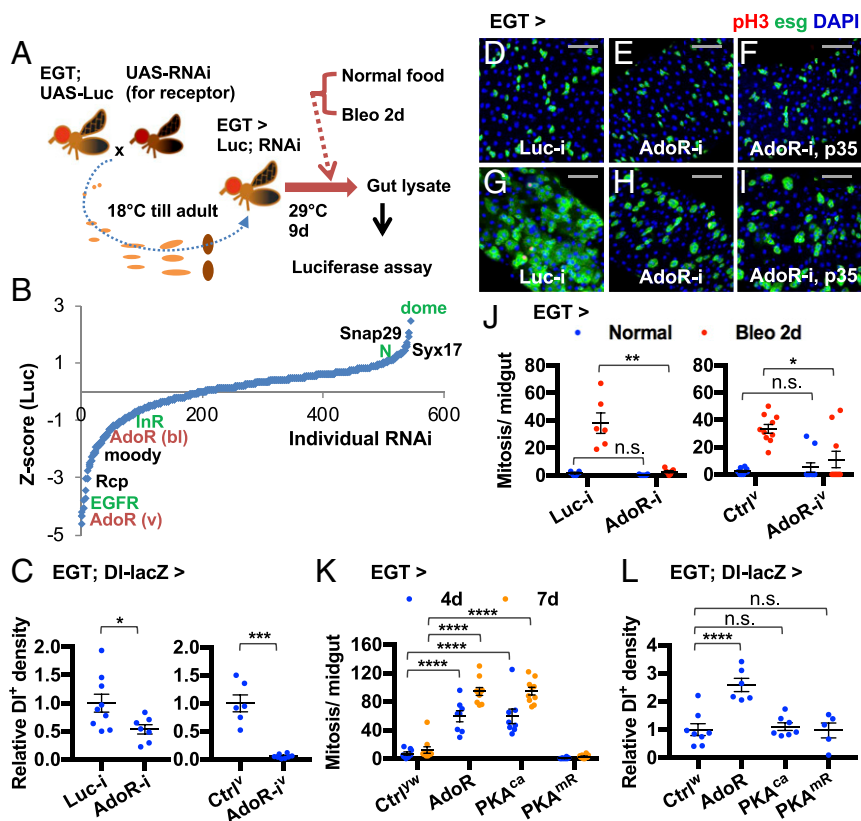


Fig. 1. Receptome RNAi screen identifies *AdoR* as a regulator of ISC proliferation and self-renewal. (A) Flowchart of the RNAi screen. Crosses were set up between *EGT; UAS-Luc* and different *UAS-RNAi* (or control) flies. Progenies were reared at 18 °C to avoid unintended RNAi expression during fly development. Young adult flies were shifted to 29 °C for 9 d to induce Luc and RNAi expression. The system is very effective at driving expression in all ISCs/EBs, as *EGT*-driven expression of the proapoptotic gene *reaper* (*rpr*) completely and irreversibly eliminates midgut mitosis (31). In addition to normal feeding, we also performed the screen under tissue-damage conditions (full results in [Dataset S1F](#)). (B) Z-score ranking plot of normalized luciferase luminescence measured from ~550 different RNAi lines (normal feeding conditions). We normalized the luciferase activity of RNAi lines from different stock centers to the average value of their respective controls spiked in the screen, i.e., *Ctrl^{bl}* for Transgenic RNAi Project (TRIP)/Bloomington Drosophila Stock Center (BDSC) stocks, *Ctrl^V* for National Institute of Genetics (NIG) stocks, and *Ctrl^V* for Vienna Drosophila Resource Center (VDRC) stocks. Each dot represents a unique RNAi line. *AdoR* RNAi lines are highlighted by red nomenclature. (C) DI^+ cell density (i.e., normalized number per area unit, relative to the controls) quantification of midguts expressing *AdoR* RNAi in ISCs/EBs for 7 d. $n = 9, 7, 6,$ and 8 midguts were analyzed for BDSC *Luc* RNAi (*Luc-i*), BDSC *AdoR* RNAi (*AdoR-i*), VDRC *Ctrl^V*, and VDRC *AdoR* RNAi (*AdoR-i^V*) groups, respectively. Data are represented as mean \pm SEM. (D–I) pH3 staining of midguts expressing *Luc-i*, *AdoR-i*, or *AdoR-i* together with *p35* in ISCs/EBs for 7 d, with or without the last 2 d on bleomycin food. (Scale bar: 50 μ m.) (J) Mitosis quantification of midguts expressing *Luc-i* ($n = 6$), *AdoR-i* ($n = 7$), *Ctrl^V* ($n = 10$), or *AdoR-i^V* ($n = 10$) in ISCs/EBs for 7 d, with or without the last 2 d on bleomycin food. Data are represented as mean \pm SEM. (K) Mitosis quantification of midguts with or without the expression of *AdoR*, *PKA^{ca}*, or *PKA^{MR}* in ISCs/EBs for 4 or 7 d. $n \geq 8$ midguts were analyzed for each group. Data are represented as mean \pm SEM. (L) DI^+ cell density quantification of midguts expressing *Ctrl^V* ($n = 8$), *AdoR* ($n = 6$), *PKA^{ca}* ($n = 7$), and *PKA^{MR}* ($n = 5$) overexpression in ISCs/EBs for 6 d. Data are represented as mean \pm SEM. * $P > 0.01 < 0.05$; ** $P > 0.001 < 0.01$; *** $P > 0.0001 < 0.001$; **** $P < 0.0001$; n.s., $P > 0.05$ is not significant.

affect the tissue-damage response ([Dataset S1G](#)), including the WNT receptor *fz2*, the alpha integrin *if*, and the beta integrin *mys*, the roles of which in the ISCs are expected based on the previous literature (8–11).

In addition to receptors, the functions of which have been characterized in ISCs/EBs, we uncovered a number of regulators of ISC activities ([Dataset S1G](#)), most of which were not identified in a previous large-scale RNAi screen of the midgut, which did not rely on a quantitative readout and focused on genes the ubiquitous knockdown of which caused developmental defects and lethality (12). First, we found that multiple RNAi lines targeting *Syx17* and *Snap29*, which encode a pair of interacting SNAP receptors that mediate the membrane fusion of autophagosomes with late endosomes and lysosomes (13), increase ISC number ([SI Appendix, Fig. S1 B–D and I–K](#)). Consistent with these RNAi phenotypes, sgRNA-directed *Syx17* or *Snap29* knockouts in ISCs/EBs increase proliferation ([SI Appendix, Fig. S1 T–W](#)). In contrast, the knockdown of genes required for the induction or early steps of autophagy such as *Atg1* or *Uba1* (14) in ISCs/EBs suppresses

proliferation ([SI Appendix, Fig. S1P](#)). Therefore, inhibition of autophagosome formation and maturation/clearance could have different signaling effects in ISCs/EBs. Second, many genes encoding neuropeptide or hormone receptors such as *moody*, *Receptor component protein* (*Rcp*), *adipokinetic hormone receptor* (*AkhR*), and *Octopamine receptor* (*Oamb*) were identified to be required for ISC maintenance and proliferation ([SI Appendix, Fig. S1 E–H, L–O, and Q and R](#)). Interestingly, *Dh31*, which encodes the *Drosophila* ortholog of the mammalian Rcp ligand calcitonin gene-related peptide (15), is expressed in a subpopulation of EEs (16). Therefore, Dh31-Rcp signaling might explain a previous report that EEs support ISC proliferation (17). Third, knockdowns of *Lipophorin receptor 2* (*LpR2*), which mediates lipid uptake (18), and *Eip75B*, which is required for *LpR* expression and lipid uptake (19), inhibit ISC proliferation ([SI Appendix, Fig. S1 P and Q](#)). The identification of genes implicated in lipid metabolism as ISC regulators might explain a previous report that the proliferation rate in the lipid-rich regions of the midgut tends to be higher than in other regions (20). Furthermore, both RNAi and

mutant phenotypes suggest the role of *Fmi*, a core component of planar cell polarity complexes, in supporting ISC activity (*SI Appendix*, Fig. S1S and Dataset S1G).

AdoR Regulates ISC Self-Renewal, Differentiation, Proliferation, and Clonal Expansion. A top candidate identified from the screen is *AdoR*, which is required to maintain the ISC/EB pool size (Fig. 1B). Expression of *AdoR* RNAi (target regions and knockdown efficiency shown in *SI Appendix*, Fig. S2A and B) in ISCs/EBs significantly decreases DI^+ cell number under homeostatic conditions (Fig. 1C, 2 different RNAi lines used), which is not due to induced cell death or differentiation, as we detected no apoptosis by staining for cleaved caspase 3 (*SI Appendix*, Fig. S2E and F), no change in Prospero-positive EEs (*SI Appendix*, Figs. S2G, H, and L), and a significant loss of the Notch pathway reporter Su(H)GFP (indicating EBs and the activity of EC differentiation) (2, 21) (*SI Appendix*, Fig. S2G, H, M, and N). ISCs/EBs expressing *AdoR* RNAi exhibit a proliferation defect, which is insignificant under homeostatic conditions when the proliferation rate is low but apparent under tissue-damage conditions (Fig. 1D–J, 2 different lines used). The inhibition of tissue-damage-induced proliferation is not due to nonspecific killing of mitotic cells as the phenotype cannot be rescued by coexpressing the antiapoptotic gene *p35* (Fig. 1F and I). Consistent with the RNAi phenotype, sgRNA-directed *AdoR* knockout in ISCs/EBs suppresses tissue-damage-induced proliferation (*SI Appendix*, Fig. S1X). Furthermore, MARCM clones generated from homozygous *AdoR* null mutant (*SI Appendix*, Fig. S1S) ISCs are much smaller than control clones. Contrary to the knockdown or knockout phenotypes, forced activation of AdoR signaling by *AdoR* overexpression (22) in ISCs/EBs stimulates ISC proliferation (Fig. 1K) and increases the number of both DI^+ cells (Fig. 1L) and Su(H)GFP⁺ cells (*SI Appendix*, Fig. S2I and J).

The *AdoR^{E02}-Gal4* line carrying ~3.1 kb putative enhancer sequences of *AdoR* (*SI Appendix*, Fig. S2A) drives gene expression ubiquitously in the midgut (*SI Appendix*, Fig. S2C). Although *AdoR* might be expressed in all cell types, *AdoR* knockdown in ISCs or EBs alone, rather than in ECs or EEs, significantly decreases tissue-damage-induced ISC proliferation (*SI Appendix*, Fig. S2D). Interestingly, *AdoR* overexpression in ISCs, rather than in EBs, causes overproliferation (*SI Appendix*, Fig. S3A–H).

PKA and Ca^{2+} /Ras/MAPK Signaling Act Downstream of AdoR to Regulate ISC Activity. AdoR belongs to the GPCR family of proteins that function mainly through the cAMP/PKA and Ras/MAPK pathways in mammals (Fig. 24). The 4 mammalian AdoR orthologs (ADORA1, ADORA2A, ADORA2B, ADORA3) regulate PKA signaling positively or negatively depending on which $G\alpha$ proteins they associate with, whereas all of them can activate Ca^{2+} and Ras/MAPK signaling via either $G\alpha$ or $G\beta\gamma$ (23, 24). Heterologous expression of *Drosophila AdoR* increases cAMP and intracellular Ca^{2+} levels in mammalian cells (22), suggesting that the signaling of *Drosophila AdoR* is similar to the mammalian orthologs.

Previously, it was reported that AdoR mediates the proliferation and differentiation of hematopoietic progenitor cells via PKA signaling in the *Drosophila* larval lymph gland (25). We stained the midguts for CRE-Luc, a reporter for the transcriptional activity of the PKA-regulated transcription factor Creb (26) and found that *AdoR* overexpression induces PKA activity in ISCs/EBs (Fig. 2B and C). Although CRE-Luc is barely detectable in the midgut epithelium under homeostatic conditions (Fig. 2B and D), an increase in CRE-Luc staining is detected in ISCs/EBs after tissue damage and the increase can be blocked by *AdoR* knockdown (Fig. 2D–G). Moreover, expression of the constitutively active PKA (*PKA^{ca}*) induces ISC proliferation (Fig. 1K) and differentiation (*SI Appendix*, Fig. S2K), whereas PKA

inhibition suppresses ISC differentiation (*SI Appendix*, Fig. S2N and O).

Despite the established AdoR-PKA connections and the similarity of AdoR and PKA phenotypes, certain important aspects of AdoR function in the midgut could not be explained by PKA. First, whereas *AdoR* overexpression causes massive expansion of DI^+ cells, PKA activation or inhibition in ISCs/EBs does not affect DI^+ cell number (Fig. 1L). Second, unlike *AdoR*, overexpression of *PKA catalytic subunit PKA-C1 (PKA)* in DI^+ ISCs does not cause overproliferation (*SI Appendix*, Fig. S3A–D). When expressed in both ISCs and EBs for 2d, *AdoR* can induce overproliferation but *PKA* or *PKA^{ca}* cannot (*SI Appendix*, Fig. S3W). Third, ISCs/EBs expressing *AdoR* RNAi cannot be induced to proliferate by the expression of *PKA*, *PKA^{ca}*, or PKA downstream targets such as the repressor form of the *Gli* ortholog *Ci (Ci⁷⁵)* and the active form of *Creb (Creb^{B^{act}})* (Fig. 2P–S). Moreover, dominant negative *PKA^{mR}* (Fig. 2W) prevents *AdoR*-induced overproliferation.

PKA increases ISC cell size (*SI Appendix*, Fig. S3C) and causes polarized shape with long membrane protrusions in EBs (Fig. 2P and Q, *SI Appendix*, Fig. S3G), which is consistent with a potent role in mediating ISC/EB differentiation toward ECs (27, 28). Furthermore, our lineage-tracing experiment suggests that ISCs/EBs expressing *AdoR* or *PKA^{ca}* for 3 d produce a large number of Pdm1+ ECs (*SI Appendix*, Fig. S3I–K). Accelerated EC production and the observation that *PKA^{ca}* or *AdoR* induction in ECs causes dramatic overproliferation (*SI Appendix*, Fig. S3L–O) might explain why PKA activation in ISCs/EBs for 4 d or longer can induce overproliferation. The nonautonomous effects of *PKA* or *AdoR* expression in ECs likely involve the activation of JNK signaling and the production of mitogenic JAK/Stat pathway ligands (7), as detected by midgut RT-qPCR (*SI Appendix*, Fig. S3P). Furthermore, the nonautonomous effects of *PKA* or *AdoR* depend on a large number of ECs, as *PKA^{ca}* or *AdoR* expression in EBs alone cannot induce overproliferation (*SI Appendix*, Fig. S3E–H).

Next, we investigated the role of the other signaling branch downstream of AdoR in ISC self-renewal and proliferation (Fig. 24). Calcium imaging suggests that *AdoR* knockdown suppresses intracellular Ca^{2+} levels in ISCs/EBs, whereas *AdoR* overexpression dramatically increases the number of ISCs/EBs with high Ca^{2+} levels (*SI Appendix*, Fig. S3X). Examination of Ras/MAPK activity by staining midguts with the antibody recognizing diphospho-extracellular signal-regulated kinase (dpErk) (29) suggests that *AdoR* knockdown in ISCs/EBs inhibits Ras/MAPK signaling under homeostatic conditions (Fig. 2H–K), whereas *AdoR* overexpression increases the number of ISCs/EBs with high Ras/MAPK activity (Fig. 2L and M). Previous studies demonstrated that Ca^{2+} signaling and Ras/MAPK are required for ISC self-renewal during tissue homeostasis (5, 30, 31). Forcing intracellular Ca^{2+} influx by *SERCA* knockdown or Ras/MAPK activation by expressing the constitutively active form of *Ras (Ras^{I^A})* increases the number of DI^+ ISCs (*SI Appendix*, Fig. S2P–S), which is consistent with *AdoR* and different from *PKA^{ca}* or *PKA^{mR}* overexpression. Similar to *AdoR*, *Ras^{I^A}* expression in ISCs alone can induce overproliferation (*SI Appendix*, Fig. S3D). Most importantly, the activation of Ca^{2+} and Ras/MAPK signaling by expressing *SERCA* RNAi, *Ras^{I^A}*, or constitutively active *Raf (Raf^{gof})* in ISCs/EBs induces overproliferation even in the presence of *AdoR* RNAi (Fig. 2O, R, and S), whereas *AdoR*-induced overproliferation can be rescued by reducing intracellular Ca^{2+} levels with *trpA1* RNAi (31) or inhibiting Ras/MAPK with *Ras1* RNAi (Fig. 2T–V). In conclusion, Ca^{2+} and Ras/MAPK signaling mediate the major effects of AdoR on ISC proliferation.

Since Ras/MAPK and PKA signaling appear to control different aspects of ISC proliferation and differentiation, we asked how their combinatorial activation could affect ISC activity. Strikingly, *Ras^{I^A}* coexpression with *PKA* or *PKA^{ca}* in ISCs/EBs

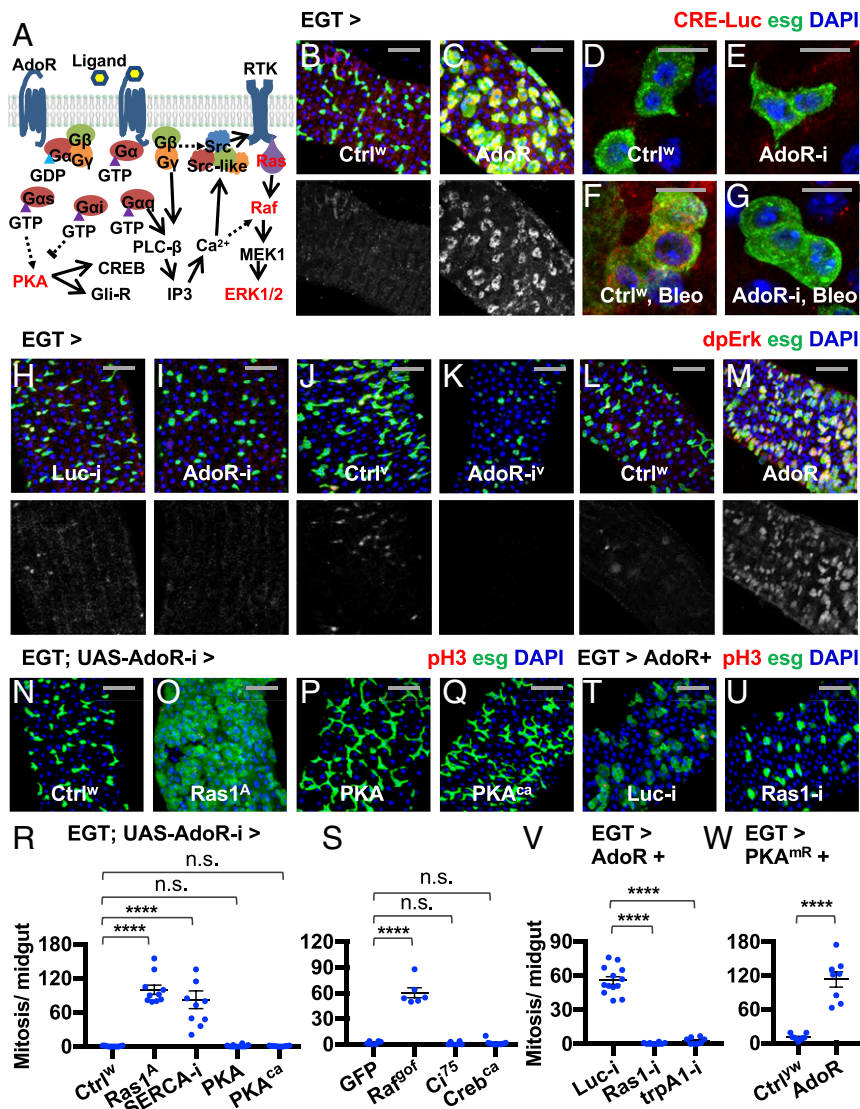


Fig. 2. Analysis of AdoR downstream signaling in the midgut. (A) Model of AdoR activation. The conformational change of AdoR, upon binding to its ligand, catalyzes the exchange of the GDP bound to G protein for a GTP, causing the dissociation of the G α subunit from the G $\beta\gamma$ heterodimer and the activation of G proteins. The 4 AdoR orthologs in mammals are known to associate with 3 major types of G α proteins that trigger different downstream signaling upon activation: G α s activate adenylyl cyclase (AC), which induces cAMP levels and PKA activity; G α i, which inhibits AC; and G α q, which activates PLC- β to stimulate Ca²⁺/Ras/MAPK signaling. In addition, G $\beta\gamma$ activates PLC- β or Src to activate Ras/MAPK. PKA activates cAMP response element-binding protein (CREB) and promotes the formation of the repressor form of Gli. (B and C) CRE-Luc staining of midguts with or without *AdoR* overexpression in ISCs/EBs for 2 d. (Scale bar: 50 μ m.) (D–G) CRE-Luc staining of midguts with or without *AdoR* RNAi expression in ISCs/EBs for 7 d with or without the last 2 d on bleomycin food. (Scale bar: 10 μ m.) (H and I) dpErk staining of midguts expressing *Luc-i* or *AdoR-i* in ISCs/EBs for 5 d. (Scale bar: 50 μ m.) The channels of dpErk stainings are presented in grayscale below the merged images in H–M. (J and K) dpErk staining of midguts with or without *AdoR-i^{iv}* expression in ISCs/EBs for 7 d. (Scale bar: 50 μ m.) (L and M) dpErk staining of midguts with or without *AdoR* overexpression in ISCs/EBs for 2 d. (Scale bar: 50 μ m.) (N–R) pH3 staining and mitosis quantification of midguts expressing *AdoR-i* alone or together with *Ras1^A*, *SERCA-i*, *PKA*, or *PKA^{ca}* in ISCs/EBs for 5 d. (Scale bar: 50 μ m.) $n \geq 10$ midguts were analyzed for each group. Data are represented as mean \pm SEM. (S) Mitosis quantification of midguts expressing *AdoR-i* together with *CD8-GFP* (control), *Raf^{90f}*, *Ci⁷⁵*, or *Creb^{9ct}* in ISCs/EBs for 5 d. $n \geq 7$ midguts were analyzed for each group. Data are represented as mean \pm SEM. (T and U) pH3 staining of midguts expressing *AdoR-i* together with *Luc-i* or *Ras1-i* RNAi in ISCs/EBs for 5 d. (Scale bar: 50 μ m.) (V) Mitosis quantification of midguts expressing *AdoR-i* together with *Luc-i* ($n = 13$), *Ras1-i* ($n = 10$), or *trpA1-i* ($n = 8$) in ISCs/EBs for 5 d. Data are represented as mean \pm SEM. (W) Mitosis quantification of midguts expressing *PKA^{MR}* alone ($n = 10$) or together ($n = 9$) with *AdoR-i* in ISCs/EBs for 5 d. Data are represented as mean \pm SEM. **** $P < 0.0001$; n.s., $P > 0.05$ is not significant.

for 2 d results in much more proliferation than the expression of *Ras1^A*, *PKA*, or *PKA^{ca}* alone (SI Appendix, Fig. S3 Q–W).

Adgf-A Produced by ECs Restricts AdoR Signaling and ISC Proliferation. Adenosine is the major ligand for AdoR. The mammalian *adenosine deaminase 2 (ADA2)* and its *Drosophila* orthologs encode secreted enzymes converting extracellular adenosine into inosine, which no longer activates AdoR (32). According to microarray

(FlyAtlas) and RNA sequencing (RNA-seq) (modENCODE) gene expression profiling data (<http://flybase.org>), *Adgf-A* is the only *Drosophila* ortholog of *ADA2* that is prominently expressed in the digestive system. To characterize *Adgf-A* expression in situ, we generated *Adgf-A-Gal4* enhancer trap flies by CRISPR/Cas9-mediated knock-in (SI Appendix, Fig. S5 A and B). *Adgf-A-Gal4* drives *mCherry* reporter expression mainly in the ECs and visceral muscles of the midgut (see Fig. 4 A and D).

To analyze *Adgf-A* function, we examined its knockdown phenotype in different midgut cell types. Strikingly, whereas flies fed with excessive adenosine exhibit normal ISC/EB number and proliferation rate, *Adgf-A* RNAi (knockdown efficiency shown in *SI Appendix*, Fig. S4 A and B) expression in ECs results in massive ISC/EB expansion and ISC overproliferation when the flies are fed with adenosine (Fig. 3 A–E). Moreover, adenosine and *Adgf-A* RNAi-induced overproliferation could be suppressed by *AdoR* knockdown in ISCs/EBs (*SI Appendix*, Fig. S4C). Consistent with EC-specific knockdown using *Myo1AGal4*, *Adgf-A* knockdown with the RU486-inducible *GSG⁹⁵²* driver (expressed mainly in ECs, as shown in *SI Appendix*, Fig. S4D) induces ISC proliferation when flies are fed with adenosine, whereas such induction of overproliferation can be inhibited by *AdoR* RNAi expression in ISCs/EBs (Fig. 3F and *SI Appendix*, Fig. S4 I–L). In contrast, *Adgf-A* knockdown in ISCs/EBs (Fig. 3F and *SI Appendix*, Fig. S4 E–H) or in visceral muscles (Fig. 3G) does not cause adenosine-induced overproliferation. In conclusion, EC-derived *Adgf-A* is required to restrict the mitogenic activity of excessive extracellular adenosine.

Adgf-A knockdown or overexpression in ECs does not affect ISC proliferation under normal feeding conditions (Figs. 3 E and F, and 4H), suggesting that *Adgf-A* does not affect the basal levels of *AdoR* activity and that there could be *Adgf-A*-independent mechanisms restricting endogenous extracellular adenosine to a minimal level in the midgut under tissue homeostatic conditions. Because various cell types can release purines, most notably ATP and adenosine, under tissue-damage or inflammation conditions (33), we investigated the expression and function of *Adgf-A* following tissue damage. Tissue damage

by bleomycin feeding drastically reduces *Adgf-A-Gal4* expression, especially in the posterior region of the midgut (Fig. 4 A and B). Quantification of *Adgf-A-Gal4*-driven *Luc* expression by luciferase assay confirms the significant decrease in midgut *Adgf-A* expression following tissue damage (Fig. 4C). A detailed examination of the posterior midgut by costaining for the *DI-lacZ* or *esg-lacZ* markers revealed that, following tissue damage, only a small fraction of ECs (as judged by large nucleus size and exclusion of progenitor markers) retain low levels of *Adgf-A* expression, whereas the expanding population of ISCs/EBs do not express *Adgf-A* (Fig. 4 A, B, D, and E). RT-qPCR measurement confirms the loss of midgut *Adgf-A* expression at the messenger RNA level (Fig. 4F). Furthermore, we used an assay that measures the rate of inosine production over time and detected a decrease of midgut adenosine deaminase activity following tissue damage (Fig. 4G).

Consistent with the role of *Adgf-A* as a proliferation suppressor in response to excessive adenosine, overexpression of *Adgf-A* in ECs under the control of either *Myo1AGal4^{ts}* or *GSG⁹⁵²* suppresses tissue-damage-induced ISC proliferation, whereas *Adgf-A* knockdown in ECs further enhances tissue-damage-induced ISC proliferation (Fig. 4 H and I). In contrast, *Adgf-A* knockdown in visceral muscles (Fig. 3G) does not affect tissue-damage-induced ISC proliferation. In addition to their degradation by the deaminase, extracellular adenosine levels are controlled by a network of channels, transporters, and enzymes (*SI Appendix*, Fig. S5C). Extracellular ATP can be dephosphorylated into adenosine via the action of membrane-bound nucleotidases or secreted alkaline phosphatase (*Alp*) (34). In addition, extracellular adenosine can originate from the direct diffusion of intracellular adenosine through equilibrative nucleoside transporters (*ENTs*) (35). To explore whether ECs are a source of extracellular adenosine, we knocked down genes required for the biogenesis of extracellular adenosine, including *Ent2* (the only *ENT* exhibiting reliable expression in the midgut, according to <http://flybase.org>), *veil* (encoding the *Drosophila* ortholog of 5'-nucleotidase, highly expressed in the midgut), and *Alp9* and *Alp10* (2 of the most highly expressed *Alps* in the midgut). Interestingly, the expression of *Ent2* RNAi, *veil* RNAi, or the simultaneous expression of *Alp9* RNAi and *Alp10* RNAi in ECs suppresses tissue-damage-induced ISC proliferation (*SI Appendix*, Fig. S5D). Altogether, our data suggest that *Adgf-A* expression is down-regulated to facilitate tissue-damage-induced proliferation and that ECs are likely a source of extracellular adenosine.

Potential Role of *ADA2*, the *Adgf-A* Ortholog, as a Tumor Suppressor.

The amino acid sequence and predicted protein structure of *Adgf-A* are highly conserved compared to its human ortholog, *ADA2* (*SI Appendix*, Fig. S5E). To analyze how *ADA2* affects the growth of human gastrointestinal epithelial cells, we chose Caco2 cells as they represent a mixture of ISC-like and EC-like cells (36) and do not carry mutations in major components of *AdoR* signaling (37). Like most colorectal cancers, Caco2 cells do not express *ADA2* (*Datset S2A*) (38). We cloned human *ADA2* into the pINDUCER20 lentiviral vector (39) and obtained a stable Caco2 cell line with doxycycline-inducible *ADA2* expression. Induced *ADA2* expression causes a moderate suppression of Caco2 cell proliferation (*SI Appendix*, Fig. S5 F and G), suggesting a conserved role of human *ADA2* as a tumor suppressor in the digestive epithelium.

Discussion

We performed an RNAi screen for regulators of ISC activity and identified *AdoR* as a gene required for Ras/MAPK and PKA signaling in the ISCs/EBs. Characterization of *AdoR* and its ligand revealed that, in the healthy midgut, EC-derived *Adgf-A* limits the bioavailability of extracellular adenosine and restricts

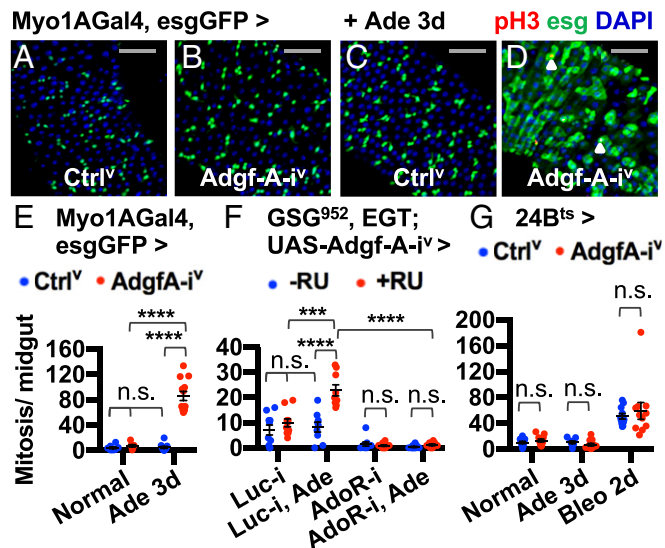


Fig. 3. EC-derived *Adgf-A* suppresses adenosine-induced ISC proliferation. (A–E) Midgut pH3 staining and mitosis quantification of flies expressing VDR *Adgf-A* RNAi (*Adgf-A-i^V*) in ECs throughout development until young adult stages (8 d post eclosion), with or without the last 3 d on food supplemented with adenosine. (Scale bar: 50 μ m.) White arrowheads highlight examples of pH3+ cells. $n \geq 7$ midguts were analyzed for each group. Data are represented as mean \pm SEM. (F) Mitosis quantification of midguts expressing *Adgf-A-i^V* together with *Luc-i* or *AdoR-i* under the control of *EGT* (ISCs/EBs) and RU486-inducible driver *GSG⁹⁵²* for 9 d with or without the last 3 d on adenosine food. $n \geq 9$ midguts were analyzed for each group. Data are represented as mean \pm SEM. (G) Mitosis quantification of midguts with or without *Adgf-A-i^V* expression in visceral muscles (under the control of *24B^{ts}*) for 8 d under normal feeding conditions with the last 3 d on food with adenosine or with the last 2 d on food with bleomycin. $n \geq 9$ midguts were analyzed for each group. Data are represented as mean \pm SEM. **** $P < 0.0001 < 0.001$; *** $P < 0.0001$; n.s., $P > 0.05$ is not significant.

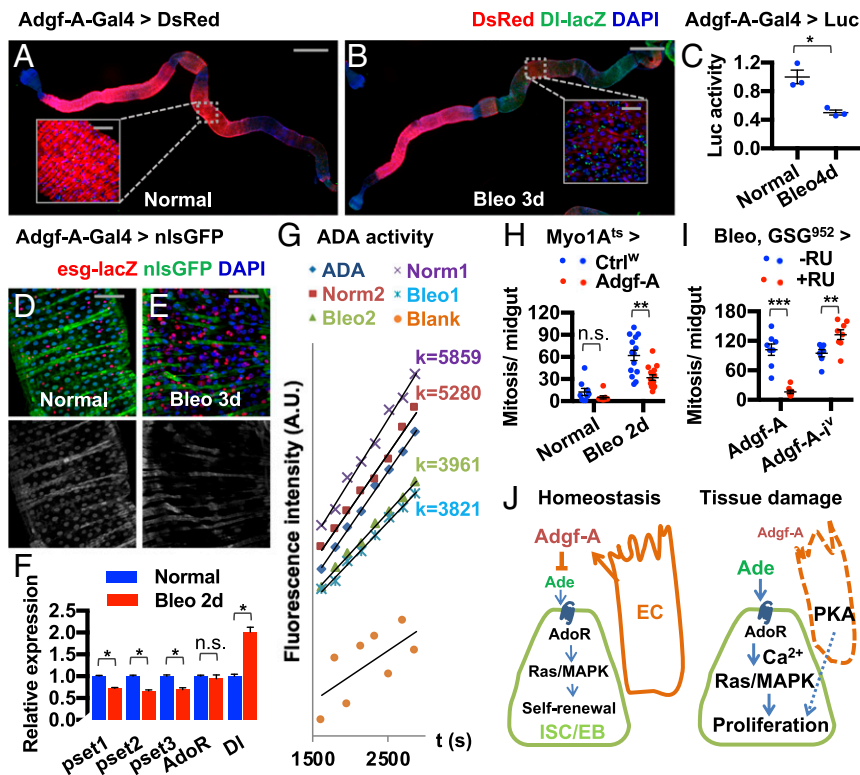


Fig. 4. Down-regulation of *Adgf-A* facilitates tissue-damage-induced ISC proliferation. (A and B) The whole gut (scale bar: 500 μ m) and zoomed-in *Inset* (scale bar: 50 μ m) corresponding to encircled posterior midgut regions views of *Adgf-A-Gal4*-driven DsRed expression in normal flies or flies fed with food containing bleomycin for 3 d. (C) Luciferase activity of midguts expressing *Luc* under the control of *Adgf-A-Gal4* with or without feeding bleomycin for 4 d before dissection. Data are represented as mean \pm SEM. (D and E) *Adgf-A-Gal4*-driven nucleus-localized GFP (nlsGFP) expression in the posterior midguts from normal flies versus flies fed with food containing bleomycin for 3 d before dissection. (Scale bar: 50 μ m.) (F) RT-qPCR measurement of *Adgf-A*, *AdoR*, or *DI* expression in midguts (genotype: *EGT*) under normal or tissue-damage conditions. Data are represented as mean \pm SEM. (G) Adenosine deaminase assay curves of wild-type midguts (genotype: *w1118*) with or without feeding bleomycin for 2 d before dissection. Two replicates of each treatment group, along with the positive (ADA) and negative (Blank) controls are presented. The kinetics of inosine production, i.e., the slope (*k* value) for the linear function of fluorescence intensity over time, indicates the activity of adenosine deaminase. (H) Mitosis quantification of midguts with or without induced *Adgf-A* overexpression in ECs for 7 d under normal or tissue damage (bleomycin feeding for 2 d) conditions. $n \geq 9$ midguts were analyzed for each group. Data are represented as mean \pm SEM. (I) Mitosis quantification of midguts with RU486-inducible overexpression or knockdown of *Adgf-A* in the midgut for 4 d on normal or RU486 food, followed by 3 d on normal or bleomycin food. $n \geq 7$ midguts were analyzed for each group. Data are represented as mean \pm SEM. (J) Schematic summary of AdoR and *Adgf-A* signaling in the midgut. Under homeostatic conditions, *Adgf-A* from healthy ECs prevents adenosine accumulation and restricts AdoR signaling to the baseline levels required for homeostatic proliferation and ISC maintenance. Following tissue damage, loss of *Adgf-A* expression allows extracellular adenosine to activate AdoR signaling. Upon AdoR activation in ISCs/EBs, Ras/MAPK signaling is induced to stimulate proliferation; PKA is also activated but not required for AdoR-driven ISC proliferation. Hyperactive PKA signaling in ECs nonautonomously stimulates ISC proliferation. * $P > 0.01 < 0.05$; ** $P > 0.001 < 0.01$; *** $P > 0.0001 < 0.001$; n.s., $P > 0.05$ is not significant.

AdoR signaling in ISCs/EBs to a baseline level that supports ISC maintenance (Fig. 4J). However, the damaged midgut lacks sufficient levels of *Adgf-A* to restrict extracellular adenosine, thus allowing the activation of AdoR and its downstream pathways to stimulate the regenerative activity of ISCs (Fig. 4J).

The Pleiotropic Effects of Extracellular Adenosine Signaling in *Drosophila* Tissues. Purines not only are required for nucleic acid synthesis and the cellular energy supply, but also represent the most primitive and common extracellular chemical messengers (40). Extracellular adenosine acts on P1-type purinergic receptors, i.e., AdoRs. The effects of AdoR signaling on cell growth are context-dependent. For example, adenosine inhibits the growth of imaginal disk cells, and *Adgf-A* was initially identified as a growth factor that stimulates the proliferation of *Drosophila* imaginal disk and embryonic cells in vitro (41). In contrast, in both larval lymph gland (25) and adult midgut (this study), *AdoR* supports proliferation and differentiation in the stem/progenitor cells whereas *AdgfA* from a nonautonomous source suppresses AdoR activity. Despite the remarkably similar roles of AdoR in controlling behaviors of 2 different types of stem/progenitor cells, AdoR

activation leads to hemopoietic progenitor exhaustion but ISC expansion. Furthermore, Ras/MAPK activity, rather than PKA (as in the hemopoietic progenitors) (25), functions as a necessary and sufficient downstream component mediating *AdoR*-induced ISC overproliferation.

Integration of PKA and Ras/MAPK Signaling in the Midgut. Identification of AdoR as an ISC regulator led us to dissect the function of its downstream pathways, i.e., PKA and Ras/MAPK. Although earlier studies reported that EC-like differentiation in *Caco2* colorectal cancer cells correlates with PKA activation (42) and that pharmacological induction of cAMP/PKA suppresses the migration of mammalian intestinal or colorectal cancer cells (43), our study implicates PKA signaling in controlling ISC behaviors in vivo. We found that PKA activation in ISCs/EBs induces ISC-EC differentiation and EB membrane elongation, whereas PKA activation in ECs nonautonomously stimulates ISC proliferation. PKA regulates cytoskeletal organizing proteins such as Rac, Cdc42, Rho, and PAK (44). Interestingly, PKA antagonizes Rac to induce morphological changes in neurons

(45). A similar mechanism might explain how PKA affects EB morphology.

Ras/MAPK activity in the ISCs/EBs is responsive to a wide spectrum of inputs, including the EGFR pathway (5), the PDGF- and VEGF-receptor-related pathway (46), and cytosolic Ca²⁺ levels (31). In this study, we confirmed AdoR as another upstream signal that can affect Ca²⁺ and Ras/MAPK activity. Since earlier studies suggested that GPCRs might affect intracellular Ca²⁺ levels (30), whereas high levels of cytosolic Ca²⁺ levels can induce Ras/MAPK activity in ISCs/EBs (31), it is likely that the detailed mechanism for AdoR to activate Ras/MAPK implicates the regulation of Ca²⁺ levels (Fig. 4J).

Following AdoR activation, both Ras/MAPK and PKA signaling are induced to facilitate ISC overproliferation and accelerated production of ECs, whereas the perdurance of PKA activity in a massive number of newly produced ECs has a synergistic effect with Ras/MAPK activity in ISCs/EBs in accelerating proliferation. Since human AdoRs are often highly expressed in carcinomas (47, 48), a similar paradigm of PKA and Ras/MAPK synergy might fuel oncogenic growth in epithelial tissues.

Relevance to Mammalian Epithelial Tissue Regeneration and Colorectal Cancers. Mammalian AdoRs and human ADA2 have been extensively studied in the hematopoietic and immune systems where ADA2 is produced by differentiating monocytes to stimulate T cell and macrophage proliferation (49, 50). Although mammalian AdoRs are expressed in human digestive epithelial cells (Dataset S2A) (38), their functions remain elusive. Different groups have reported contradictory results suggesting either a protective or a pathological role of AdoR signaling during tissue damage in the mouse intestine (51), which could be due to the differences in mouse culture conditions, genetic backgrounds, damage models, or inflammation responses. Therefore, our study in *Drosophila* might help clarify the function of AdoR signaling in the digestive epithelium and in epithelial stem cells.

In carcinomas, *ADA2* is focally and frequently deleted, based on copy number analysis (summarized in Dataset S2B) (52). Deleterious *ADA2* mutations have been identified in colorectal cancers in The Cancer Genome Atlas (TCGA) and Catalogue of Somatic Mutations in Cancer projects (Dataset S2 C–E). Moreover, *ADA2* expression is significantly down-regulated in colorectal cancers, according to microarray studies and RNA-seq datasets from TCGA (Dataset S2F). Further, anti-*ADA2* stainings were detected in the normal digestive epithelium but not in colorectal cancers (Dataset S2G) (38). Therefore, the down-regulation of *ADA2* in colorectal carcinomas has been observed at DNA, RNA, and protein levels. Unfortunately, *ADA2* cannot be studied in a mouse model because of a rodent-specific gene loss event during evolution (based on <http://asia.ensembl.org/index.html>). Moreover, murine developmental and physiological programs have adapted to the loss of *ADA2*, as transgenic expression of human *ADA2* in mice results in abnormal development

and embryonic/neonatal lethality (53). Therefore, our findings describe a striking case in which flies are uniquely suited for understanding the function and regulation of an important disease-related gene.

Materials and Methods

Detailed materials and methods, including *Drosophila* stocks and culture, generation of transgenic and recombinant flies, staining and imaging, mRNA quantification, Luciferase and adenosine deaminase assay, mammalian cell culture and analysis, and statistical methods are in *SI Appendix*.

Generation of Knock-In Flies via sgRNA/Cas9-Mediated Genome Editing. To generate *Adgf-A-Gal4* knock-in flies, we cloned a single sgRNA targeting *Adgf-A* translational start site (seed sequence: ATGACTGGCGACATGATGAGCGG) into the U6-sgRNA vector pCFD3 and generated a Gal4 version of the pH-DsRed donor vector (54) with ~1-kb homology arms on each end. Approximately 10 micrograms sgRNA and ~10 µg donor vectors were mixed with 400 µL Qiagen PB buffer (Qiagen catalog no.19066), transferred to QIAprep Spin columns, centrifuged at 7,000 × g for 30 s, washed with 700 µL Qiagen PE buffer (Qiagen catalog no.19065) twice, and spun for another 60 s to remove residual liquid. The plasmids were eluted with 70 µL injection buffer (5 mM KCl, 100 µM sodium phosphate buffer with pH 6.8) and injected into embryos expressing Cas9 (genotype: *nanos-Cas9/CyO*). After homologous recombination, the Gal4 fragment (including SV40 polyA sequences) along with the 3xP3-DsRed fluorescent selection marker is expected to insert at the endogenous start codon of *Adgf-A*. This approach is extremely efficient: within ~50 embryos injected and 15 fertile parental generation flies (P0) obtained, 2 were prominently fluorescent and 9 were mosaics. We could successfully identify fluorescent F1 progenies to establish stable knock-in stocks from 11 of the 15 P0 flies. The loxP-flanked 3xP3-DsRed fluorescent reporter used to screen for knock-in flies is subsequently removed by crossing to flies that ubiquitously express the Cre recombinase (*hsp70-Mos1-Cre*). Knock-in stocks were confirmed by genotyping PCR using 2 pairs of primers (forward and reverse): gtPCR1—AGTGCAATTGGATGCTGATG and AGCGGAGACCTTTGGTTTT and gtPCR2—CACACCAATTGCCTCTCT and AATGCGCACAGTATCCATAGG.

Data Availability. All data are available within this manuscript and the associated *SI Appendix*.

ACKNOWLEDGMENTS. We thank the Transgenic RNAi Project and Bloomington *Drosophila* Stock Center for providing fly stocks; the Microscopy Resources on the North Quad core (Harvard Medical School) for imaging support; Michelle Markstein, Utpal Banerjee, Jerry Yin, Daniel Calderon, Bruce Edgar, Gary Struhl, and Ruth Lehmann for sharing fly stocks; Kate O'Connor-Giles for pH-DsRed vector; Sida Liao and Steve Elledge for pINDUCER20 lentiviral vector; Laura Fredenburgh for Caco2 cells; Xuming Zhou and Gladyshev Vadim for discussions; the N.P. laboratory members, especially Mary-Lee Dequeant, Wei Song, and Li He for discussion and technical instructions; Andrey Parkhitko for the help with RU486 food; Jonathan DiRusso and Richard Binari for help maintaining fly stocks; and Afroditi Petsakou and Rueil-Jiun Hung for comments on the manuscript. Work in the N.P. laboratory is supported by the National Institute of General Medical Sciences (Grant GM067761), the Starr Cancer Consortium, and Howard Hughes Medical Institute (HHMI). Work in the X.H. laboratory is supported by NIH Grant R01-DK121945. N.P. is an Investigator of the HHMI. H.-W.T. is supported by the Human Frontier Science Program. X.H. is an American Cancer Society Research Professor.

1. B. Ohlstein, A. Spradling, The adult *Drosophila* posterior midgut is maintained by pluripotent stem cells. *Nature* **439**, 470–474 (2006).
2. C. A. Michelli, N. Perrimon, Evidence that stem cells reside in the adult *Drosophila* midgut epithelium. *Nature* **439**, 475–479 (2006).
3. H. Jiang, B. A. Edgar, Intestinal stem cells in the adult *Drosophila* midgut. *Exp. Cell Res.* **317**, 2780–2788 (2011).
4. A. Amcheslavsky, J. Jiang, Y. T. Ip, Tissue damage-induced intestinal stem cell division in *Drosophila*. *Cell Stem Cell* **4**, 49–61 (2009).
5. H. Jiang, M. O. Grenley, M.-J. Bravo, R. Z. Blumhagen, B. A. Edgar, EGFR/Ras/MAPK signaling mediates adult midgut epithelial homeostasis and regeneration in *Drosophila*. *Cell Stem Cell* **8**, 84–95 (2011).
6. N. H. Choi, E. Lucchetta, B. Ohlstein, Nonautonomous regulation of *Drosophila* midgut stem cell proliferation by the insulin-signaling pathway. *Proc. Natl. Acad. Sci. U.S.A.* **108**, 18702–18707 (2011).
7. H. Jiang et al., Cytokine/Jak/Stat signaling mediates regeneration and homeostasis in the *Drosophila* midgut. *Cell* **137**, 1343–1355 (2009).
8. G. Lin, N. Xu, R. Xi, Paracrine Wingless signalling controls self-renewal of *Drosophila* intestinal stem cells. *Nature* **455**, 1119–1123 (2008).
9. J. B. Cordero, R. K. Stefanatos, A. Scopelliti, M. Vidal, O. J. Sansom, Inducible progenitor-derived Wingless regulates adult midgut regeneration in *Drosophila*. *EMBO J.* **31**, 3901–3917 (2012).
10. S. Goulas, R. Conder, J. A. Knoblich, The Par complex and integrins direct asymmetric cell division in adult intestinal stem cells. *Cell Stem Cell* **11**, 529–540 (2012).
11. G. Lin et al., Integrin signaling is required for maintenance and proliferation of intestinal stem cells in *Drosophila*. *Dev. Biol.* **377**, 177–187 (2013).
12. X. Zeng et al., Genome-wide RNAi screen identifies networks involved in intestinal stem cell regulation in *Drosophila*. *Cell Rep.* **10**, 1226–1238 (2015).
13. S. Takáts et al., Autophagosomal Syntaxin17-dependent lysosomal degradation maintains neuronal function in *Drosophila*. *J. Cell Biol.* **201**, 531–539 (2013).
14. T. K. Chang et al., Uba1 functions in Atg7- and Atg3-independent autophagy. *Nat. Cell Biol.* **15**, 1067–1078 (2013).

15. E. C. Johnson *et al.*, A novel diuretic hormone receptor in *Drosophila*: Evidence for conservation of CGRP signaling. *J. Exp. Biol.* **208**, 1239–1246 (2005).
16. J. Chen, S. M. Kim, J. Y. Kwon, A systematic analysis of *Drosophila* regulatory peptide expression in enteroendocrine cells. *Mol. Cells* **39**, 358–366 (2016).
17. A. Amcheslavsky *et al.*, Enteroendocrine cells support intestinal stem-cell-mediated homeostasis in *Drosophila*. *Cell Rep.* **9**, 32–39 (2014).
18. E. Parra-Peralbo, J. Culi, *Drosophila* lipophorin receptors mediate the uptake of neutral lipids in oocytes and imaginal disc cells by an endocytosis-independent mechanism. *PLoS Genet.* **7**, e1001297 (2011).
19. M. H. Sieber, A. C. Spradling, Steroid signaling establishes a female metabolic state and regulates SREBP to control oocyte lipid accumulation. *Curr. Biol.* **25**, 993–1004 (2015).
20. A. Marianes, A. C. Spradling, Physiological and stem cell compartmentalization within the *Drosophila* midgut. *eLife* **2**, e00886 (2013).
21. B. Ohlstein, A. Spradling, Multipotent *Drosophila* intestinal stem cells specify daughter cell fates by differential notch signaling. *Science* **315**, 988–992 (2007).
22. E. Dolezelova, H. P. Nothacker, O. Civelli, P. J. Bryant, M. Zurovec, A *Drosophila* adenosine receptor activates cAMP and calcium signaling. *Insect Biochem. Mol. Biol.* **37**, 318–329 (2007).
23. L. Antonioli, C. Blandizzi, P. Pacher, G. Haskó, Immunity, inflammation and cancer: A leading role for adenosine. *Nat. Rev. Cancer* **13**, 842–857 (2013).
24. N. Mitin, K. L. Rossman, C. J. Der, Signaling interplay in Ras superfamily function. *Curr. Biol.* **15**, R563–R574 (2005).
25. B. C. Mondal *et al.*, Interaction between differentiating cell- and niche-derived signals in hematopoietic progenitor maintenance. *Cell* **147**, 1589–1600 (2011).
26. M. P. Belvin, H. Zhou, J. C. Yin, The *Drosophila* dCREB2 gene affects the circadian clock. *Neuron* **22**, 777–787 (1999).
27. Z. A. Antonello, T. Reiff, E. Ballesta-Illan, M. Dominguez, Robust intestinal homeostasis relies on cellular plasticity in enteroblasts mediated by miR-8-Escargot switch. *EMBO J.* **34**, 2025–2041 (2015).
28. C. Xu *et al.*, The septate junction protein Tsp2A restricts intestinal stem cell activity via endocytic regulation of aPKC and Hippo signaling. *Cell. Rep.* **26**, 670–688.e6 (2019).
29. L. Gabay, R. Seger, B. Z. Shilo, In situ activation pattern of *Drosophila* EGF receptor pathway during development. *Science* **277**, 1103–1106 (1997).
30. H. Deng, A. A. Gerencser, H. Jasper, Signal integration by Ca²⁺ regulates intestinal stem-cell activity. *Nature* **528**, 212–217 (2015).
31. C. Xu, J. Luo, L. He, C. Montell, N. Perrimon, Oxidative stress induces stem cell proliferation via TRPA1/RyR-mediated Ca²⁺ signaling in the *Drosophila* midgut. *eLife* **6**, e22441 (2017).
32. S. A. Maier, L. Podemski, S. W. Graham, H. E. McDermid, J. Locke, Characterization of the adenosine deaminase-related growth factor (ADGF) gene family in *Drosophila*. *Gene* **280**, 27–36 (2001).
33. G. Burnstock, Purinergic signalling. *Br. J. Pharmacol.* **147** (suppl. 1), S172–S181 (2006).
34. M. Pettengill *et al.*, Soluble ecto-5'-nucleotidase (5'-NT), alkaline phosphatase, and adenosine deaminase (ADA1) activities in neonatal blood favor elevated extracellular adenosine. *J. Biol. Chem.* **288**, 27315–27326 (2013).
35. S. L. Tilley, R. C. Boucher, A1 antagonism in asthma: Better than coffee? *J. Clin. Invest.* **115**, 13–16 (2005).
36. M. Rousset, The human colon carcinoma cell lines HT-29 and Caco-2: Two in vitro models for the study of intestinal differentiation. *Biochimie* **68**, 1035–1040 (1986).
37. D. Chisanga *et al.*, Colorectal cancer atlas: An integrative resource for genomic and proteomic annotations from colorectal cancer cell lines and tissues. *Nucleic Acids Res.* **44**, D969–D974 (2016).
38. M. Uhlen *et al.*, Towards a knowledge-based human protein atlas. *Nat. Biotechnol.* **28**, 1248–1250 (2010).
39. K. L. Meerbrey *et al.*, The pINDUCER lentiviral toolkit for inducible RNA interference in vitro and in vivo. *Proc. Natl. Acad. Sci. U.S.A.* **108**, 3665–3670 (2011).
40. G. Burnstock, A. Verkhatsky, Evolutionary origins of the purinergic signalling system. *Acta Physiol. (Oxf.)* **195**, 415–447 (2009).
41. M. Zurovec, T. Dolezal, M. Gazi, E. Pavlova, P. J. Bryant, Adenosine deaminase-related growth factors stimulate cell proliferation in *Drosophila* by depleting extracellular adenosine. *Proc. Natl. Acad. Sci. U.S.A.* **99**, 4403–4408 (2002).
42. S. Pignata, L. Maggini, R. Zarrilli, A. Rea, A. M. Acquaviva, The enterocyte-like differentiation of the Caco-2 tumor cell line strongly correlates with responsiveness to cAMP and activation of kinase A pathway. *Cell Growth Differ.* **5**, 967–973 (1994).
43. N. P. Zimmerman, S. N. Kumar, J. R. Turner, M. B. Dwinell, Cyclic AMP dysregulates intestinal epithelial cell restitution through PKA and RhoA. *Inflamm. Bowel Dis.* **18**, 1081–1091 (2012).
44. A. K. Howe, Regulation of actin-based cell migration by cAMP/PKA. *Biochim. Biophys. Acta* **1692**, 159–174 (2004).
45. A. Goto, Y. Kamioka, M. Matsuda, PKA modulation of Rac in neuronal cells. *Front. Cell. Neurosci.* **8**, 321 (2014).
46. D. Bond, E. Foley, Autocrine platelet-derived growth factor-vascular endothelial growth factor receptor-related (Pvr) pathway activity controls intestinal stem cell proliferation in the adult *Drosophila* midgut. *J. Biol. Chem.* **287**, 27359–27370 (2012).
47. C. Sepúlveda, I. Palomo, E. Fuentes, Role of adenosine A2b receptor overexpression in tumor progression. *Life Sci.* **166**, 92–99 (2016).
48. L. Madi *et al.*, The A3 adenosine receptor is highly expressed in tumor versus normal cells: Potential target for tumor growth inhibition. *Clin. Cancer Res.* **10**, 4472–4479 (2004).
49. G. Haskó, J. Linden, B. Cronstein, P. Pacher, Adenosine receptors: Therapeutic aspects for inflammatory and immune diseases. *Nat. Rev. Drug Discov.* **7**, 759–770 (2008).
50. A. V. Zavalov *et al.*, Human adenosine deaminase 2 induces differentiation of monocytes into macrophages and stimulates proliferation of T helper cells and macrophages. *J. Leukoc. Biol.* **88**, 279–290 (2010).
51. S. P. Colgan, B. Fennimore, S. F. Ehrentraut, Adenosine and gastrointestinal inflammation. *J. Mol. Med. (Berl.)* **91**, 157–164 (2013).
52. R. Beroukhi *et al.*, The landscape of somatic copy-number alteration across human cancers. *Nature* **463**, 899–905 (2010).
53. A. M. Riazi, G. Van Arsdell, M. Buchwald, Transgenic expression of CECR1 adenosine deaminase in mice results in abnormal development of heart and kidney. *Transgenic Res.* **14**, 333–336 (2005).
54. S. J. Gratz *et al.*, Highly specific and efficient CRISPR/Cas9-catalyzed homology-directed repair in *Drosophila*. *Genetics* **196**, 961–971 (2014).